OPEN

Citation: Cell Death and Disease (2017) 8, e2793; doi:10.1038/cddis.2017.202
Official journal of the Cell Death Differentiation Association

www.nature.com/cddis

Acyl-CoA thioesterase 7 is involved in cell cycle progression via regulation of PKCζ–p53–p21 signaling pathway

Seung Hee Jung[1,2], Hyung Chul Lee[1,2], Hyun Jung Hwang[1,2], Hyun A Park[1], Young-Ah Moon[1], Bong Cho Kim[3], Hyeong Min Lee[4], Kwang Pyo Kim[4], Yong-Nyun Kim[5], Byung Lan Lee[6], Jae Cheol Lee[7], Young-Gyu Ko[8], Heon Joo Park[2,9] and Jae-Seon Lee*[,1,2]

Acyl-CoA thioesterase 7 (ACOT7) is a major isoform of the ACOT family that catalyzes hydrolysis of fatty acyl-CoAs to free fatty acids and CoA-SH. However, canonical and non-canonical functions of ACOT7 remain to be discovered. In this study, for the first time, ACOT7 was shown to be responsive to genotoxic stresses such as ionizing radiation (IR) and the anti-cancer drug doxorubicin in time- and dose-dependent manners. ACOT7 knockdown induced cytostasis via activation of the p53–p21 signaling pathway without a DNA damage response. PKCζ was specifically involved in ACOT7 depletion-mediated cell cycle arrest as an upstream molecule of the p53–p21 signaling pathway in MCF7 human breast carcinoma and A549 human lung carcinoma cells. Of the other members of the ACOT family, including ACOT1, 4, 8, 9, 11, 12, and 13 that were expressed in human, ACOT4, 8, and 12 were responsive to genotoxic stresses. However, none of those had a role in cytostasis via activation of the PKCζ–p53–p21 signaling pathway. Analysis of the ACOT7 prognostic value revealed that low ACOT7 levels prolonged overall survival periods in breast and lung cancer patients. Furthermore, ACOT7 mRNA levels were higher in lung cancer patient tissues compared to normal tissues. We also observed a synergistic effect of ACOT7 depletion in combination with either IR or doxorubicin on cell proliferation in breast and lung cancer cells. Together, our data suggest that a low level of ACOT7 may be involved, at least in part, in the prevention of human breast and lung cancer development via regulation of cell cycle progression.
Cell Death and Disease (2017) **8,** e2793; doi:10.1038/cddis.2017.202; published online 18 May 2017

Acyl-CoA thioesterases (ACOTs) are enzymes that catalyze hydrolysis of fatty acyl-CoAs to free fatty acids and CoA-SH. ACOTs are expressed ubiquitously in prokaryotes and eukaryotes.[1] In higher organisms, different ACOT isoforms are localized to distinct cellular organelles, including peroxisomes, endoplasmic reticulum, cytosol and mitochondria. ACOTs have various chain length specificities on fatty acyl-CoAs and are distributed across a wide range of mammalian tissues.[2–4] To date, 13 mammalian genes have been identified as ACOT superfamily members,[2,3,5] and they are highly regulated by peroxisome proliferator-activated receptors (PPARs) and other nutritional factors.[1] Although their physiological functions remain incompletely understood, recent gene knockout and in-depth characterization studies have revealed that a subgroup of ACOTs profoundly affect lipid metabolism and cellular signaling.[4,6–9] ACOTs are broadly grouped into two classes based on enzyme molecular weight.[2] Despite catalyzing the same reaction, these two classes are not structurally similar and do not share sequence homology.[3,10] Type 1 enzymes (ACOTs 1–6) are localized to the cytosol (ACOT1), mitochondria (ACOT2), and peroxisomes (ACOT3–ACOT6).[9,11–13] The larger (>100 kDa of molecular weight) oligomeric type II ACOTs (ACOTs 7–13) have different cellular localizations depending on the isoform.[9,10,14]

ACOT7 (also known as BACH, CTE-II, ACT, ACH1, and BACHa) is one of the most extensively studied ACOTs as a major isoform of the ACOT family.[9] The enzyme is localized to the cytosol and is highly expressed in brain tissue and testis,[15,16] showing a preference for long-chain acyl-CoA substrates with fatty acid chains of 8–16 carbon atoms (C8–C16).[17,18] ACOT7 is primarily implicated in the hydrolysis of arachidonyl-CoA (AA-CoA) to arachidonic acid (AA) and CoA. AA is an important precursor molecule for proinflammatory eicosanoids and plays a number of important cellular roles in cell signaling, regulation of cell proliferation, and activation of metabolic enzymes.[9,19,20] ACOT7 has recently been identified as playing a role in neurotoxic prevention through regulation of neuronal fatty acid metabolism.[21] Forwood *et al.* demonstrated that ACOT7 is a candidate drug target in inflammatory disease, as overexpression of ACOT7 was shown to alter production of prostaglandins D2 and E2 in a macrophage cell line.[9,22] However, the roles of ACOT7 under various stressful conditions remain to be further revealed.

Protein kinase C (PKC) is involved in a variety of cellular functions, including cell proliferation, malignant proliferation,

[1]Department of Molecular Medicine, Inha University College of Medicine, Incheon, Korea; [2]Hypoxia-Related Disease Research Center, Inha University College of Medicine, Incheon, Korea; [3]Division of Basic Radiation Bioscience, Korea Institute of Radiological and Medical Sciences, Seoul, Korea; [4]Department of Applied Chemistry, College of Applied Science, Kyung Hee University, Yongin, Korea; [5]Division of Cancer Biology, Research Institute, National Cancer Center, Goyang, Korea; [6]Department of Anatomy, Seoul National University College of Medicine, Seoul, Korea; [7]Department of Oncology, Asan Medical Center, College of Medicine, University of Ulsan, Seoul, Korea; [8]Division of Life Sciences, Korea University, Seoul, Korea and [9]Department of Microbiology, Inha University College of Medicine, Incheon, Korea
*Corresponding author: J-S Lee, Department of Molecular Medicine, Inha University College of Medicine, Incheon 22212, Korea. Tel: +82 32 860 0942; Fax: +82 32 885 8302; E-mail: jaeslee@inha.ac.kr
Received 13.10.16; revised 14.3.17; accepted 06.4.17; Edited by M Agostini

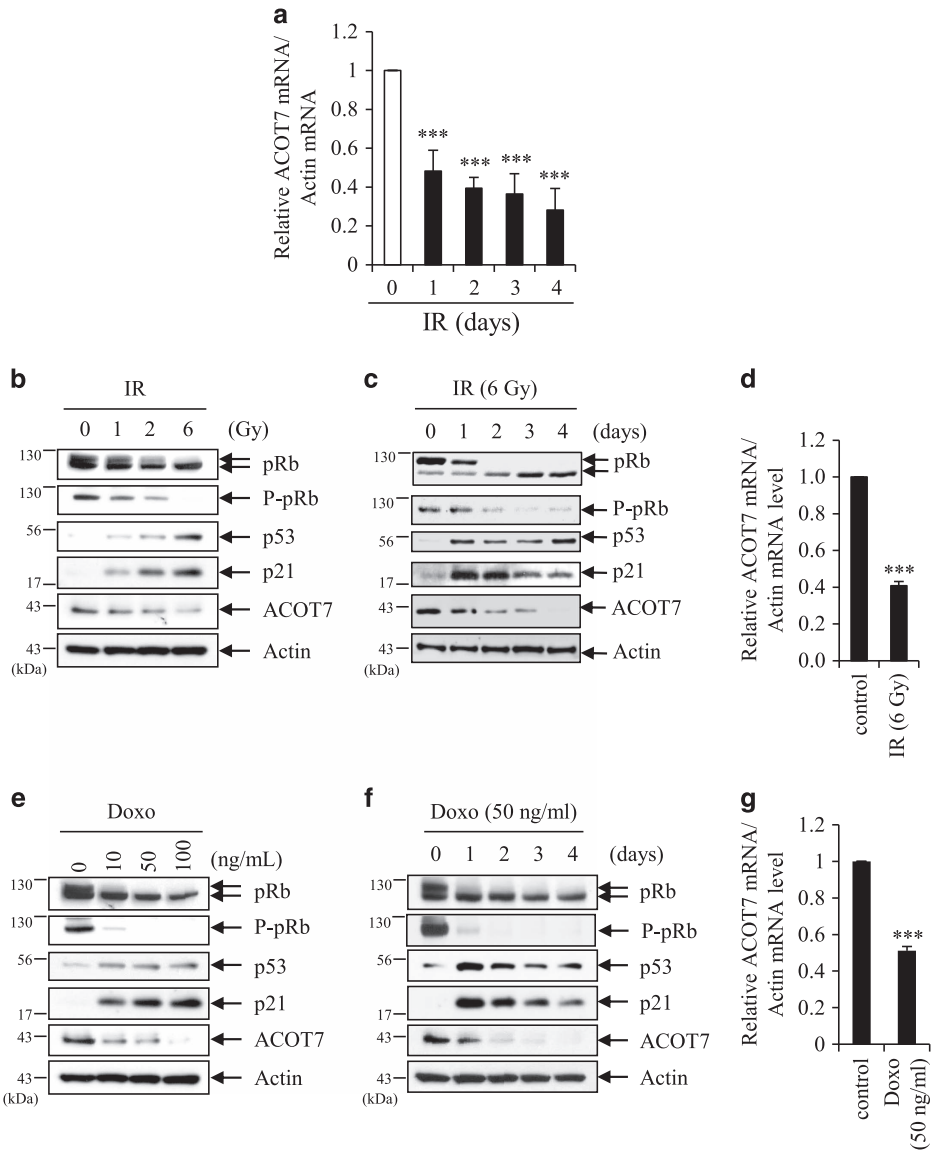

Figure 1 ACOT7 is downregulated in IR-exposed and Doxo-treated cells. (**a**) Reduction of ACOT7 in IR-exposed MCF7 cells. Cells were exposed to 6 Gy of IR and harvested at the indicated time, followed by microarray. Levels of ACOT7 mRNA in IR-exposed cells were compared with that of the unexposed control group. (**b** and **c**) MCF7 cells were exposed to IR at doses of 1, 2, and 6 Gy and harvested 2 days after irradiation (**b**) or exposed to 6 Gy of IR and harvested on the indicated days after irradiation (**c**), followed by immunoblotting. Actin was used as a loading control. (**d**) MCF7 cells were irradiated with 6 Gy of IR, incubated for 2 days, and then harvested for qRT-PCR analyses. (**e** and **f**) MCF7 cells were treated with 10, 50, and 100 ng/ml of Doxo and harvested 2 days after treatment (**e**) or treated with 50 ng/ml of Doxo and harvested on the indicated days after treatment (**f**), followed by immunoblot analysis. Actin was used as a loading control. (**g**) MCF7 cells were treated with 50 ng/ml of Doxo, incubated for 2 days, and then harvested for qRT-PCR analyses. The values represent the mean ± S.D. of three independent experiments. *** Indicates the statistical significance of $P<0.001$ by Student's *t*-test

differentiation, and cell death.[23] The PKC family is composed of at least 10 serine–threonine kinases based on their structural components and activation mechanism, and they are subdivided into three groups in mammals: classical or calcium-dependent (PKC*α*, *β*1, *β*2, and *γ*), novel or calcium-independent (PKC*δ*, *ε*, *η*, and *θ*), and atypical (PKC*ζ* and *λ*/ι). Classical PKCs are activated by oncogenic Kras or growth factors, leading to similar downstream signaling for control of cancer cell survival and metastasis.[24] Among novel PKCs, whereas PKC*ε* and PKC*δ* have been implicated in cancer development or progression, relatively little is known about PKC*η* and PKC*θ*.[25–28] Atypical PKCs are structurally and functionally distinct from other PKCs. PKC*ζ* and PKC*λ*/ι as atypical PKCs have 84% amino-acid sequence homology in their kinase domains and contain a distinct N-terminal structural domain called Phox/Bem1 (PB1) that is specific for this subfamily.[29,30] PKC*ζ* and PKC*λ*/ι do not seem to be functionally redundant and cannot compensate for each other.[31] All PKC isoforms share a highly conserved catalytic domain and more divergent regulatory domain.[32] These relatively less conserved regulatory domains have different structures that affect the sensitivity of each PKC to various stimuli. PKCs seem to be involved in all aspects of tumorigenesis, including initiation, progression, and

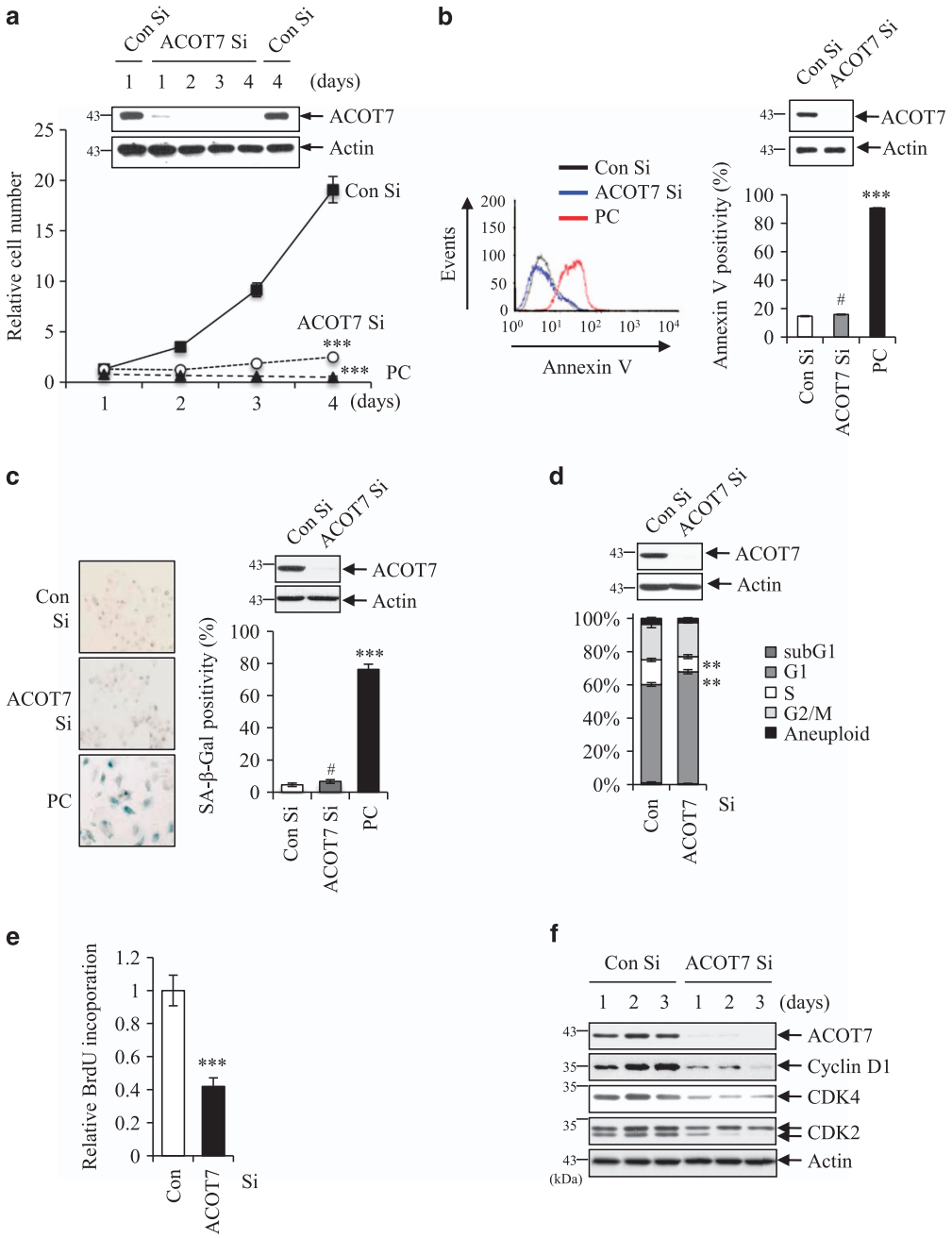

Figure 2 Depletion of ACOT7 induces cell cycle arrest. (**a**) Relative numbers of viable cells were determined on the indicated days after transfection of 100 nM ACOT7 Si into MCF7 cells. Viable cell numbers on 1 day after transfection was considered as 1. Cells treated with Doxo (5 μg/ml) were used as a positive control (PC). Total protein was extracted from cells the indicated days after siRNA transfection and was subjected to WB analysis. (**b**) Percentages of positive cells for Annexin V staining were determined in MCF7 cells transfected with Con Si and ACOT7 Si using fluorescence-activated cell sorting (FACS) 1 day after transfection. Cells treated with Doxo (5 μg/ml) were used as a PC for apoptosis. (**c**) Positivity for SA-β-Gal staining was evaluated at 4 days after transfection of either Con Si or ACOT7 Si into MCF7 cells. Cells exposed to IR (6 Gy) were used as a PC for SA-β-Gal staining. (**d**) Cells were harvested 3 days after transfection with Con Si and ACOT7 Si, and FACS was used to analyze cell cycle distribution. (**e**) DNA synthesis rates of MCF7 cells with ACOT7 depletion were measured based on BrdU incorporation into cells. (**f**) Whole-cell lysates were prepared from cells transfected with Con Si and ACOT7 Si on the indicated days after transfection. Immunoblotting was performed. Actin served as a loading control. The values represent the mean $\pm$ S.D. of three independent experiments. ***, **, and # indicate the statistical significance of $P<0.001$, $P<0.01$, and $P>0.05$ by Student's *t*-test, respectively, comparing to cells transfected with either Con Si

metastasis.[33] The existence of various PKC isoforms suggests specialized roles for isoforms in the control of cellular functions.[34] For example, whereas PKCε induces cell proliferation, PKCδ inhibits growth. Further studies should elucidate the molecular mechanism of each PKC isoform in relation to cellular functions.

In this study, we observed downregulation of ACOT7 upon treatment with genotoxic stresses such as ionizing radiation

(IR) and doxorubicin (Doxo). We found that ACOT7 depletion induced cytostasis through the PKCζ–p53–p21 signaling pathway. Furthermore, we demonstrated the synergistic effect of ACOT7 depletion and treatment with either IR or Doxo on cancer cell proliferation, suggesting ACOT7 might be a novel target for anti-cancer therapy.

Results

ACOT7 is downregulated in cells exposed to IR or Doxo. To examine changes in the gene expression profile of irradiated cancer cells, we conducted gene expression analysis of an IR-exposed MCF7 human breast carcinoma.[35]

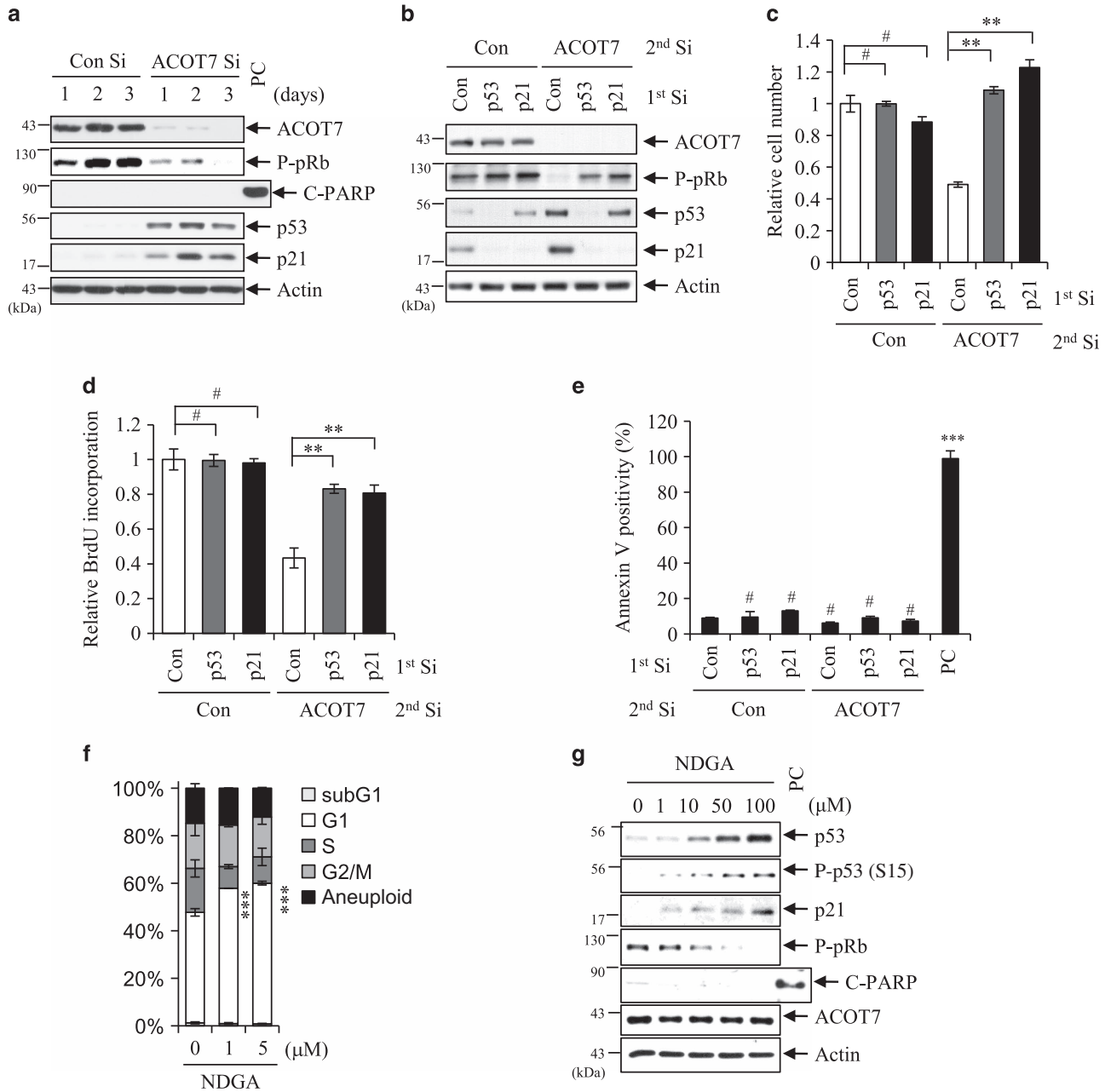

Figure 3 Cell cycle arrest mediated by ACOT7 depletion requires p53 and p21. (**a**) MCF7 cells were transfected with Con Si and ACOT7 Si. Cells were harvested on the indicated days after transfection. Actin was used as a loading control. (**b**) MCF7 cells were transfected with Con Si, p53 Si, or p21 Si. On the next day, half of each group was transfected with Con Si while the other half was transfected with ACOT7 Si. Two days after the second transfection, whole-cell extracts were prepared from cells, and immunoblotting was performed. Actin served as a loading control. (**c**) Relative numbers of viable cells were determined 4 days after transfection with the indicated siRNAs. (**d**) BrdU incorporation rates were determined in cells transfected with the indicated siRNAs. (**e**) FACS of siRNA-transfected cells was used to assess percentages of Annexin V-positive cells. (**f** and **g**) MCF7 cells were harvested 3 days after NDGA (acyl-CoA thioesterase inhibitor) treatment. FACS was used to analyze the cell cycle distribution (**f**), and immunoblotting was performed (**g**). Cells treated with 5 μg/ml of Doxo served as a PC. The values represent the mean ± S.D. of three independent experiments. ***, **, and # indicate the statistical significance of $P<0.001$, $P<0.01$, and $P>0.05$ by Student's *t*-test, respectively

Gene expression analysis showed that ACOT7 expression markedly decreased in IR-exposed MCF7 cells (Figure 1a). To verify downregulation of ACOT7 upon IR exposure, MCF7 cells were exposed to various doses of IR (1, 2, and 6 Gy), and protein levels of ACOT7 were measured using western blot analysis. Levels of ACOT7 protein decreased in IR-exposed MCF7 cells in dose- and time-dependent manners (Figures 1b and c). From the qRT-PCR results, reduction of ACOT7 mRNA expression was confirmed in IR-exposed cells (Figure 1d). To determine whether or not ACOT7 expression was altered after treatment with the anti-cancer drug Doxo, we measured ACOT7 mRNA and protein levels in Doxo-treated MCF7 cells. Levels of ACOT7 protein were also reduced in Doxo-treated cells in dose- and time-dependent manners (Figures 1e and f). ACOT7 mRNA expression also evidently decreased in Doxo-treated MCF7 cells (Figure 1g). When we assessed apoptotic cells with Annexin V positivity, the applied doses of IR (1, 2, and 6 Gy) and of low concentration Doxo (10, 50, and 100 ng/ml) did not significantly induce apoptosis compared to that in 5 μg/ml Doxo-treated cells as a positive control (Supplementary Figure S1). To determine whether other ACOT family members could be induced by IR or Doxo treatment, we examined the changes in expression levels of ACOT1, 4, 8, 9, 11, 12, and 13 which are expressed in human, as is ACOT7.[2] ACOT4 and 12 were overexpressed and ACOT8 was underexpressed in IR- and Doxo-treated MCF7 cells (Supplementary Figure S2a).

ACOT7 depletion induces cytostasis via p53–p21 signaling pathway. Next, we assessed the effect of ACOT1, 4, 7, 8, 9, 11, 12, and 13 knockdown and their effects on relative cell numbers in MCF7 cells (Supplementary Figures S2b and c). As shown in Supplementary Figure S2c, only ACOT7 depletion produced a marked decrease of relative cell numbers, although ACOT9 showed a slight decrease of relative cell numbers. Thus, we transfected siRNA against ACOT7 (ACOT7 Si) into MCF7 cells and further observed the effect of ACOT7 depletion on cell proliferation and survival. MCF7 cells treated with ACOT7 Si decreased in number compared with Control siRNA (Con Si) treatment up to 4 days (Figure 2a). Reduction of cell number could be primarily attributed to induction of apoptosis or cellular senescence or cytostasis. MCF7 cells transfected with ACOT7 Si did not show elevation of Annexin V positivity (marker of apoptosis) (Figure 2b). High concentration of Doxo (1 μg/ml) was used as a positive control (PC) of apoptosis (Figures 2a and b). Next, we examined whether or not ACOT7 depletion could trigger cellular senescence. Positivity of SA-β-galactosidase (SA-β-Gal), a marker of cellular senescence, was not affected by ACOT7 depletion, in contrast to the PC group showing induction of cellular senescence upon 6 Gy of IR exposure (Figure 2c). ACOT7-depleted MCF7 cells exhibited a higher proportion of cells in G1 phase as well as less cells in S phase (Figure 2d). BrdU incorporation was reduced to 40% of that of the control (Con) group (Figure 2e). Consistent with these results, proteins involved in cell cycle regulation such as cyclin D1, cyclin-dependent kinase 2 (CDK2), and CDK4 were also downregulated in ACOT7-depleted cells (Figure 2f). These results demonstrate that ACOT7-depleted cells underwent cytostasis rather than apoptosis or cellular senescence. However, when ACOT7 was overexpressed in MCF7 cells, cell morphology (Supplementary Figure S3a), cell number (Supplementary Figure S3b), and levels of phosphorylated pRb (P-pRb), p53, and p21 (Supplementary Figure S3c) were not affected.

Depletion of ACOT7 in MCF7 cells was accompanied by p53 and p21 accumulation in close correlation with reduction of P-pRb (Figure 3a). Poly (ADP-ribose) polymerase (PARP) cleavage as a marker of apoptosis was not detected, consistent with the results of Figure 2b. To determine whether or not cytostasis in ACOT7-depleted cells was directly correlated with either p53 accumulation or p21 induction, we knocked down either p53 or p21 prior to ACOT7 depletion using specific siRNAs (Figure 3b). Induction of p21 was completely dependent on p53 activation in ACOT7-depleted cells (Figure 3b). While depletion of ACOT7 alone markedly decreased cell number, depletion of ACOT7 in combination with either p53 Si or p21 Si rescued cell number up to that of the control group (Figure 3c). Depletion of either p53 or p21 alone did not significantly affect relative cell number compared to the control group (Figure 3c). BrdU incorporation was closely correlated with relative cell numbers in p53- and p21-depleted cells in the presence or absence of ACOT7 (Figure 3d). Under such conditions, Annexin V positivity was not affected (Figure 3e). We also observed a dramatic decrease in cell numbers in ACOT7-depleted A549 human lung carcinoma cells due to cycle arrest compared to Con Si-treated cells (Supplementary Figures S4a and b). ACOT7-depleted A549 cells exhibited hypo-phosphorylation of pRb and activation of the p53/p21 signaling pathway (Supplementary Figure S4c).

ACOT7 is a cytosolic acyl coenzyme A thioester hydrolase that primarily hydrolyzes the CoA thioester of palmitoyl-CoA. To determine whether or not ACOT7 depletion-mediated cytostasis is due to acyl-CoA thioesterase activity *per se*, we treated MCF7 cells with nordihydroguaiaretic acid (NDGA), an inhibitor of Acyl-CoA thioesterase.[36] NDGA treatment resulted in cell cycle arrest in G1 phase (Figure 3f). NDGA treatment induced hypophosphorylation of pRb as well as p53 and p21 accumulation but no detectable PARP cleavage in dose-dependent manner (Figure 3g). These results indicate that loss of Acyl-CoA thioesterase activity could trigger the p53–p21 signaling pathway, resulting in cell cycle arrest in cancer cells.

We further examined whether the DNA damage response is triggered during ACOT7 depletion-induced cytostasis. We performed western blot analyses with anti-phospho ATM and anti-gamma-H2AX antibodies to detect the DNA damage response in ACOT7-depleted MCF7 cells. ACOT7 depletion did not change the phosphorylation status of ATM or γ-H2AX at short (1, 8, and 24 h) and longer (1, 2, and 3 d) period time intervals (Figures 4a and d). In contrast, phosphorylations of ATM and γ-H2AX were detected in both 6 Gy of IR-exposed and 50 ng/ml Doxo-treated positive control groups (Figures 4b and c). We also examined γ-H2AX foci in nucleus, an indicator of DNA damage, with confocal microscope. In contrast to IR-exposed cells, ACOT7 Si-transfected cells did not exhibit gamma-H2AX foci in the nucleus (Figure 4e). These results indicate that ACOT7 depletion induces cytostasis in the absence of a DNA damage response.

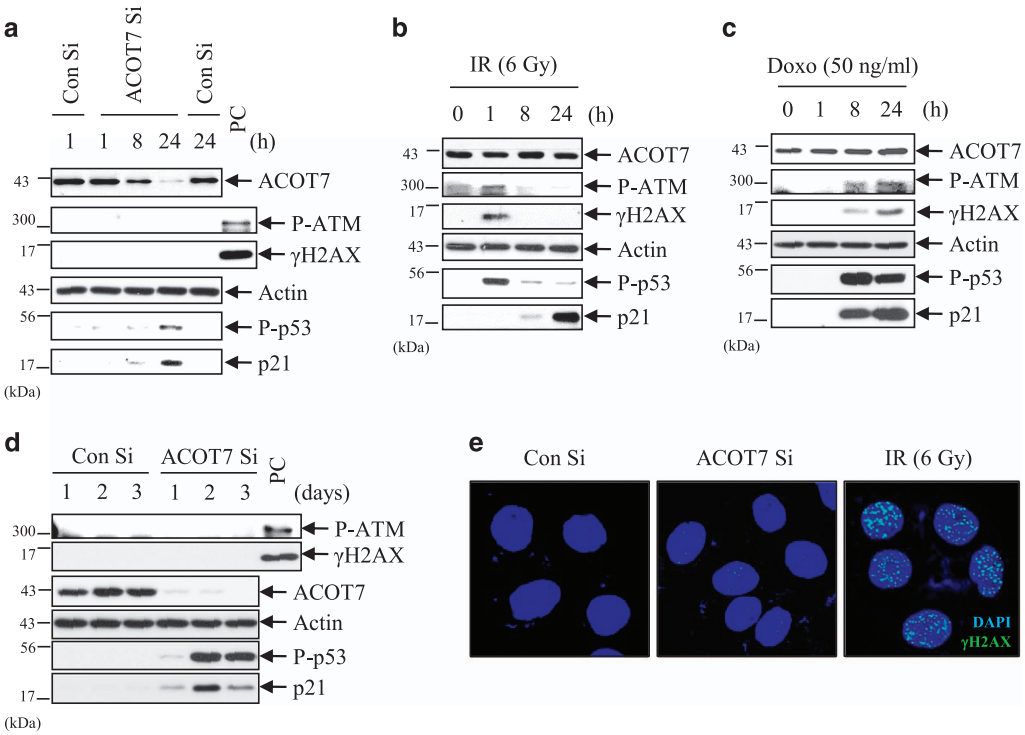

Figure 4 The DNA damage response is not involved in ACOT7 depletion-mediated cytostasis. (**a**–**d**) After transfection of ACOT7 Si (**a** and **d**), or after exposure to 6 Gy IR (**b**), or after treatment with 50 ng/ml Doxo (**c**), MCF7 cells were harvested at the indicated time intervals. Western blotting analysis was performed with anti-phospho ATM and anti-γH2AX. (**e**) Immunocytochemical staining of γH2AX (green) was conducted at 1 day after transfection of ACOT7 Si. DNA was counterstained with DAPI (blue). Cells exposed to 6 Gy of IR were used as the positive control (PC)

PKCζ is involved in ACOT7 depletion-mediated cell cycle arrest. Next, we identified which upstream molecule induced p53 activation under ACOT7-depleted conditions. ACOT7 produces arachidonic acid (AA) and CoA-SH from arachidonoyl-CoA.[37] and AA production might be associated with PKC activity.[20,38,39] To determine whether or not PKC activity is involved in activation of the p53–p21 signaling pathway induced by ACOT7 depletion, we analyzed the phosphorylation status of several PKC subtypes. While phosphorylation of PKCα/β and δ/θ was not altered by ACOT7 depletion, PKCζ phosphorylation was evidently induced in ACOT7-depleted cells (Figure 5a). To rule out the possibility of an off-target effect of ACOT7 Si, we transfected another ACOT7 Si sequence (ACOT7 #2). We confirmed a lack of off-target effects of ACOT7 Si in pRb hypo-phosphorylation, p53–p21 accumulation, and PKCζ activation (Supplementary Figure S4d). We also observed PCKζ phosphorylation as well as pRb hypo-phosphorylation and activation of the p53/p21 signaling pathway in ACOT7-depleted A549 cells (Supplementary Figure S4c). To examine direct involvement of PKCζ in activation of the p53–p21 signaling pathway induced by ACOT7 depletion, we co-transfected PKCζ Si and ACOT7 Si into MCF7 cells. We failed to detect hypo-phosphorylation of pRb and activation of the p53–p21 signaling pathway in ACOT7 and PKCζ double knock downed cells (Figure 5b). While cells transfected with ACOT7 Si showed decreased cell numbers and cell cycle arrest in G1 phase, cells co-transfected with ACOT7 Si and PKCζ Si recovered relative cell numbers and were released from cell cycle arrest in G1 phase compared with either control cells or PKCζ-alone transfected cells (Figures 5c and d).

Next, we investigated whether, in addition to ACOT7, other isoforms of ACOT family members including ACOT1, 4, 8, 9, 11, 12, and 13 are also able to activate the PCKζ–p53–p21 signaling pathway and induce cell cycle arrest (Supplementary Figure S2d). In contrast to the effect of ACOT7 depletion, depletion of other ACOT family members did not affect phosphorylation of PKCζ nor induced activation of the p53–p21 signaling pathway (Supplementary Figure S2d). Among the tested ACOT family members, hypophosphorylation of pRb was the most evident in ACOT7-depleted cells. ACOT9 depletion showed p21 accumulation and ACO11 depletion induced PKCα/β phosphorylation. These results indicate that ACOT7 depletion induced cell cycle arrest specifically through activation of the PKCζ–p53–p21 signaling pathway; other members of the ACOT family did not.

ACOT7 plays role as anti-tumor therapeutic target. To explore the biological significance of the critical role of ACOT7 in cell cycle progression, we evaluated the prognostic value of ACOT7 expression using microarray data from patients with breast cancer (http://kmplot.com/analysis/). Patients with low ACOT7 levels showed longer overall survival periods than breast cancer patients with high ACOT7 levels (Figure 6a). We also analyzed gene expression data

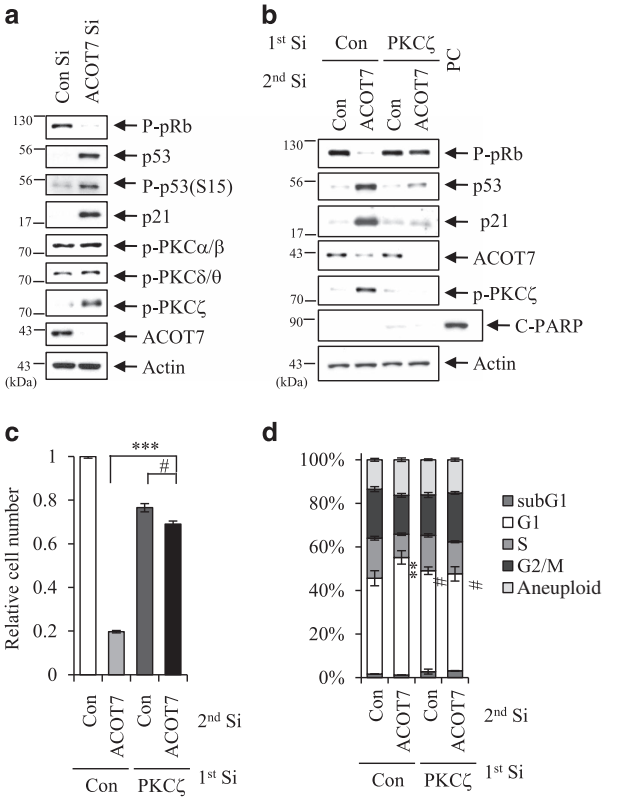

Figure 5 Activation of PKCζ is involved in cell cycle arrest induced by ACOT7 depletion. (**a**) Cells were harvested 2 days after transfection with PKCζ Si, after which immunoblotting was performed. Actin served as a loading control. (**b**–**d**) MCF7 cells were transfected with Con Si or PKCζ Si. On the next day, cells were transfected with Con Si or ACOT7 Si. Transfected cells were harvested for immunoblotting (**b**), the relative numbers of viable cells (**c**), and FACS analysis for cell cycle distribution (**d**) in cells transfected with the indicated siRNAs. Two days of transfection, immunoblotting and FACS analysis were conducted. Actin served as a loading control. Four days after transfection, viable cells were counted and compared with that of the control group, which is 1. Cells treated with 5 μg/ml of Doxo served as a PC. The values represent the mean ± S.D. of three independent experiments. *** and # indicate statistical significance of $P<0.001$ and $P>0.05$ by Student's *t*-test, respectively

from the Cancer Genome Atlas and observed upregulated ACOT7 expression in carcinoma breast tissues compared with normal breast tissues (Figure 6b). To evaluate the anti-tumor effect of ACOT7 depletion in combination with IR in breast carcinoma cells, ACOT7 was depleted in MCF7 cells using siRNA prior to exposure to 2 Gy of IR. As shown, effects of ACOT7 Si in combination with 2 Gy of IR on cell growth and clonogenicity were more effective than 2 Gy of IR (PC) alone (Figures 6c and d). Downregulation of ACOT7 by transfection of ACOT7 Si in combination with 2 Gy of IR exposure further increased accumulation of p53 and p21 via PKCζ activation comparing to 2 Gy of IR alone (Figure 6e). We also examined the anti-tumor effect of ACOT7 depletion in combination with Doxo (10 ng/ml) and found that combined ACOT7 Si and Doxo treatment increased anti-cancer drug sensitivity as well as accumulation of p53 and p21 via PKCζ activation in MCF7 cells (Figures 6f–h).

Low ACOT7 levels also prolonged overall survival periods in lung cancer patients based on analysis of the ACOT7 prognostic value (http://kmplot.com/analysis/) (Figure 7a). Furthermore, we assessed mRNA levels of ACOT7 in lung cancer patient tissues. We collected cancerous and corresponding normal tissue samples from nine lung cancer patients diagnosed with adenocarcinoma, bronchioalveolar carcinoma, or squamous cell carcinoma. Relative mRNA expression levels were analyzed using qRT-PCR (Figure 7b). Cancer tissues exhibited higher ACOT7 mRNA levels than normal tissues ($P=0.0052$; data are presented as mean ± S.E.M.). To assess the anti-tumor effect of ACOT7 depletion in combination with either IR or Doxo, we measured relative cell numbers and clonogenicity in ACOT7-depleted A549 human lung carcinoma cells. As shown, ACOT7 depletion induced tumor sensitivity either to IR (Figures 7c and d) or Doxo (Figures 7e and f). Furthermore, we evaluated the anti-tumoral effect of NDGA treatment in combination with IR or Doxo in MCF7 breast carcinoma cells. As shown in Figure 8, NDGA treatment enhanced the effect of IR or Doxo on cell growth and clonogenicity comparing with IR- or Doxo-alone-treated cells (Figures 8a and b). In addition, combination treatments of NDGA with either IR or Doxo were augmented PKCζ–p53–p21 signaling pathway (Figures 8c and d). We also examined the anti-tumoral effect of NDGA treatment in combination with IR or Doxo in A549 lung carcinoma cells, and found the enhanced anti-tumoral effects comparing to IR- or Doxo-alone-treated cells (Figures 8e and f). Altogether, these results indicate that a decreased ACOT7 activity may be involved, at least in part, in prevention of human breast and lung cancer development via regulation of cell cycle progression.

Discussion

Radiotherapy and chemotherapy are the most effective therapeutic regimes along with surgery for cancer treatment.[40] Many studies have focused on increasing tumor sensitivity to IR and chemotherapeutic drugs. We have also tried to identify genes that are specifically involved in cellular responses to IR and chemotherapeutic drugs.[35,41,42] Here we observed that ACOT7 was responsive to DNA damaging stimuli such as IR and Doxo in breast and lung carcinoma cells (Figure 1). When we transfected ACOT7 Si alone, cancer cell proliferation was markedly inhibited via activation of the PKCζ–p53–p21 signaling pathway (Figure 2). In addition, treatment with ACOT7 Si in combination with either IR or Doxo further sensitized cancer cells through augmentation of the PKCζ–p53–p21 signaling pathway (Figures 6 and 7). ACOT7 depletion as well as the acyl-CoA thioesterase inhibitor NDGA induced cell cycle arrest through induction of p53–p21 accumulation (Figure 3), indicating that acyl-CoA thioesterase activity *per se* might be involved in cell cycle regulation.

PKC is a family of serine/threonine kinases with at least 10 isoforms. The PKC family has been identified as a key player that orchestrates downstream signaling pathways regulating apoptosis and cell survival.[23,43–45] However, PKC has a striking feature that individual isoforms can exert either similar or opposite effects in cellular processes. Moreover, although PKCs are the key enzymes involving in p53 phosphorylation, PKC isoforms differentially regulate p53 activity.[34] In this study,

PKCζ was found to be specifically involved in ACOT7-mediated p53 activation, p21 accumulation, and cell cycle arrest, whereas PKCα/β and δ/θ were not (Figure 4). Our results support that PKC isoforms differentially regulate p53 activity and have their own specific features in cellular processes.

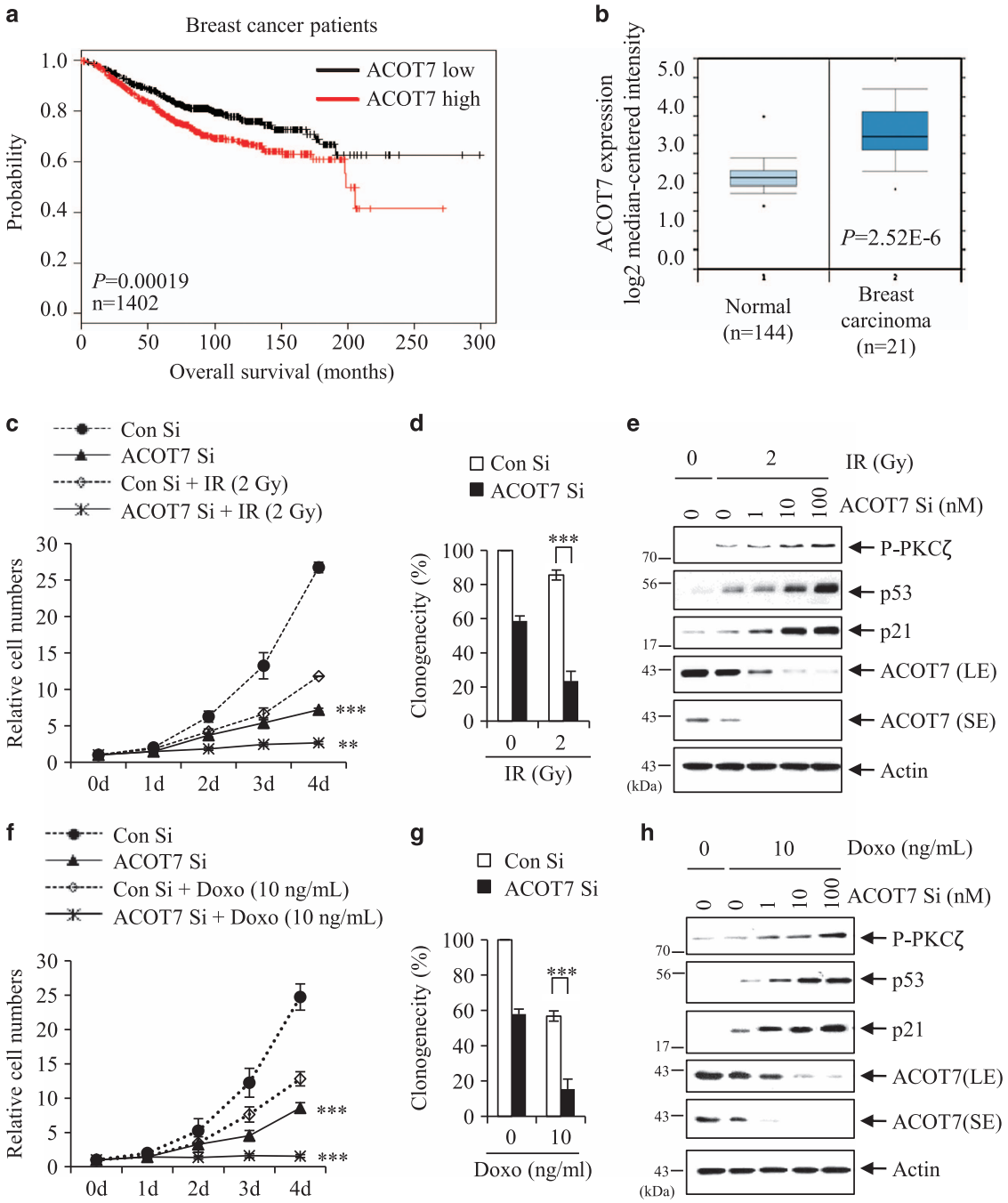

Figure 6 ACOT7 depletion sensitizes breast cancer cells to irradiation and anti-cancer drug. (**a**) Kaplan–Meier curves of overall survival times of patients with breast cancer. Data were obtained from http://kmplot.com/analysis/. Statistical significance was determined using the log-rank test. (**b**) Box plots comparing ACOT7 expression (as log2 median-centered ratios) in normal breast and carcinoma breast tissues. Dots indicate extreme data values. Data were obtained from http://oncomine.org/. (**c** and **d**) MCF7 cells were transfected with Con Si or 10 nM ACOT Si prior to 2 Gy of IR exposure. Relative cell numbers were determined on the indicated days (**c**). Colony-forming assay was performed after 7 days (**d**). (**e**) Immunoblot analysis were performed on MCF7 cells transfected with ACOT7 Si indicated concentrations and exposed to 2 Gy of IR. Actin was used as a loading control. (**f** and **g**) MCF7 cells were transfected with Con Si or 10 nM ACOT Si prior to treatment with 10 ng/ml of Doxo. Relative cell number was determined on the indicated days (**f**). Colony-forming assay was performed after 7 days (**g**). (**h**) Immunoblot analysis was performed in MCF7 cells transfected with ACOT7 Si and then treated with 10 ng/ml of Doxo for 2 days. Actin was used as a loading control. SE and LE indicates short and long exposures, respectively. The value represents the mean ± S.D. from three independent experiments. *** and ** indicate statistical significance of $P<0.001$ and $P<0.01$ by Student's *t*-test, respectively

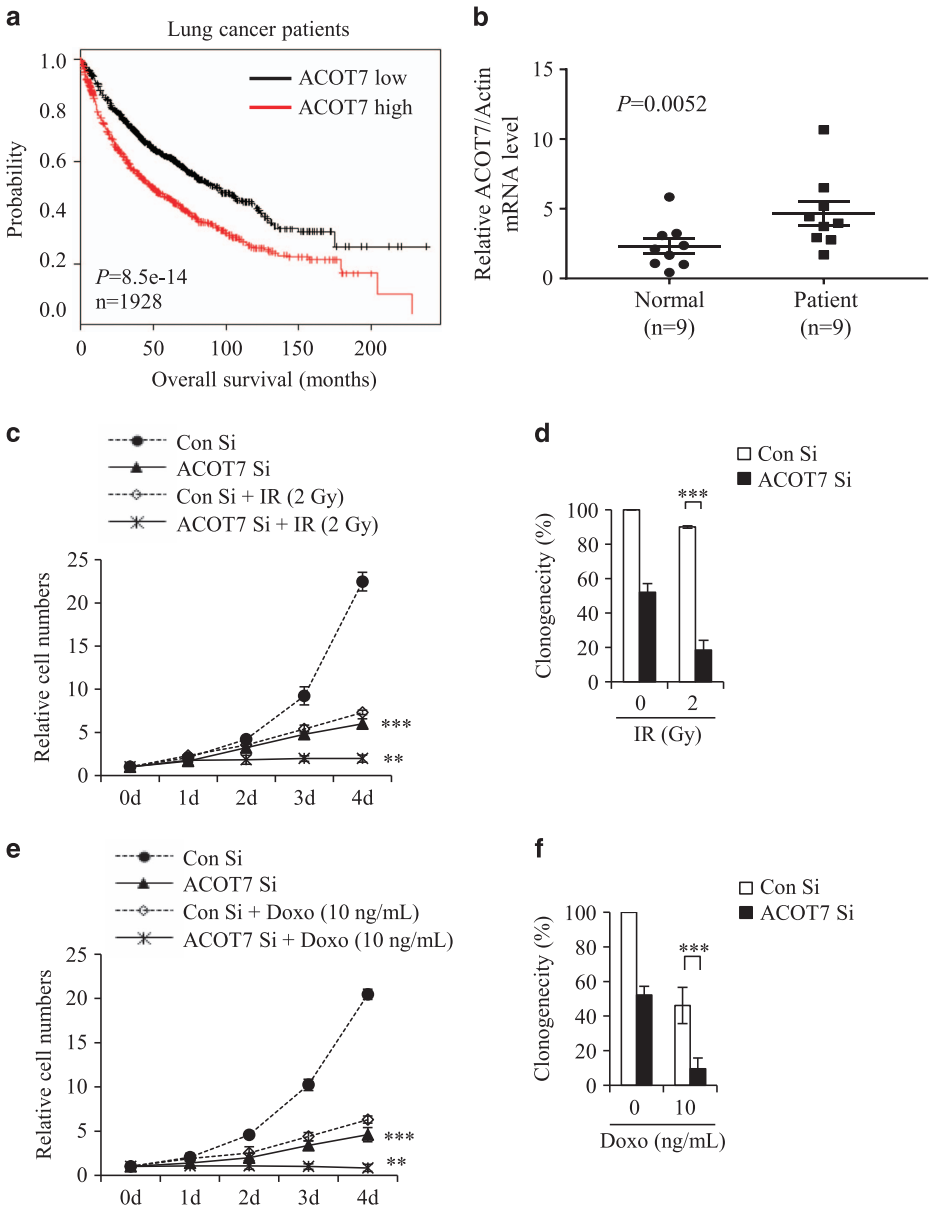

Figure 7 Effect of ACOT7 depletion in irradiated and anti-cancer drug-treated lung cancer cells and patients. (**a**) Kaplan–Meier curves of overall survival times of patients with lung cancer. Data were obtained from http://kmplot.com/analysis/. Statistical significance was determined using the log-rank test. (**b**) Quantitative RT-PCR analysis of ACOT7 mRNA in patient tissues. RNA was purified from lung cancer tissues and corresponding normal counterparts from nine patients and subjected to qRT-PCR using ACOT7-specific primers. Expression levels were normalized to actin mRNA. Error bars represent ± S.E.M. (**c** and **d**) A549 cells were transfected with Con Si or 10 nM ACOT Si prior to exposure to 2 Gy of IR. Relative cell numbers were determined on the indicated days (**c**). Colony-forming assay was performed after 7 days (**d**). (**e** and **f**) A549 cells were transfected with Con Si or 10 nM ACOT Si prior to treatment with 10 ng/ml of Doxo. Relative cell numbers were determined on the indicated days (**e**). Colony-forming assay was performed after 7 days (**f**). The value represents the mean ± S.D. from three independent experiments. *** and ** indicate statistical significance of $P<0.001$ and $P<0.01$ by Student's *t*-test, respectively

ACOTs regulate lipid metabolism by modulating cellular levels of activated fatty acids (acyl-CoAs), free fatty acids, and CoA.[1] The ACOT family consists of 13 mammalian genes and is divided into two subfamilies base on enzyme weight.[2,3] Type I ACOTs comprise the smaller group, which contains only four genes: ACOT1, ACOT2, ACOT4, and ACOT6 in human. ACOT3 and ACOT5 are found in both mouse and rat.[3] ACOT1 and ACOT2 are the most closely related, having 98% amino-acid sequence identity. ACOT6 mRNA is not detected in human tissue, and only a truncated version of the protein could be expressed by using of recombinant clone.[2] Type II ACOTs are strikingly less related than type I proteins. ACOT10 has only been identified in mice. Within the ACOT enzyme family, in particular, ACOT7 has been identified as having an important function in inflammatory reactions through production of AA.[2] It was proposed that ACOT7-mediated AA production may provide a complementary source of AA to the well-characterized phospholipase A_2 (PLA_2) pathway.[9,46] The high

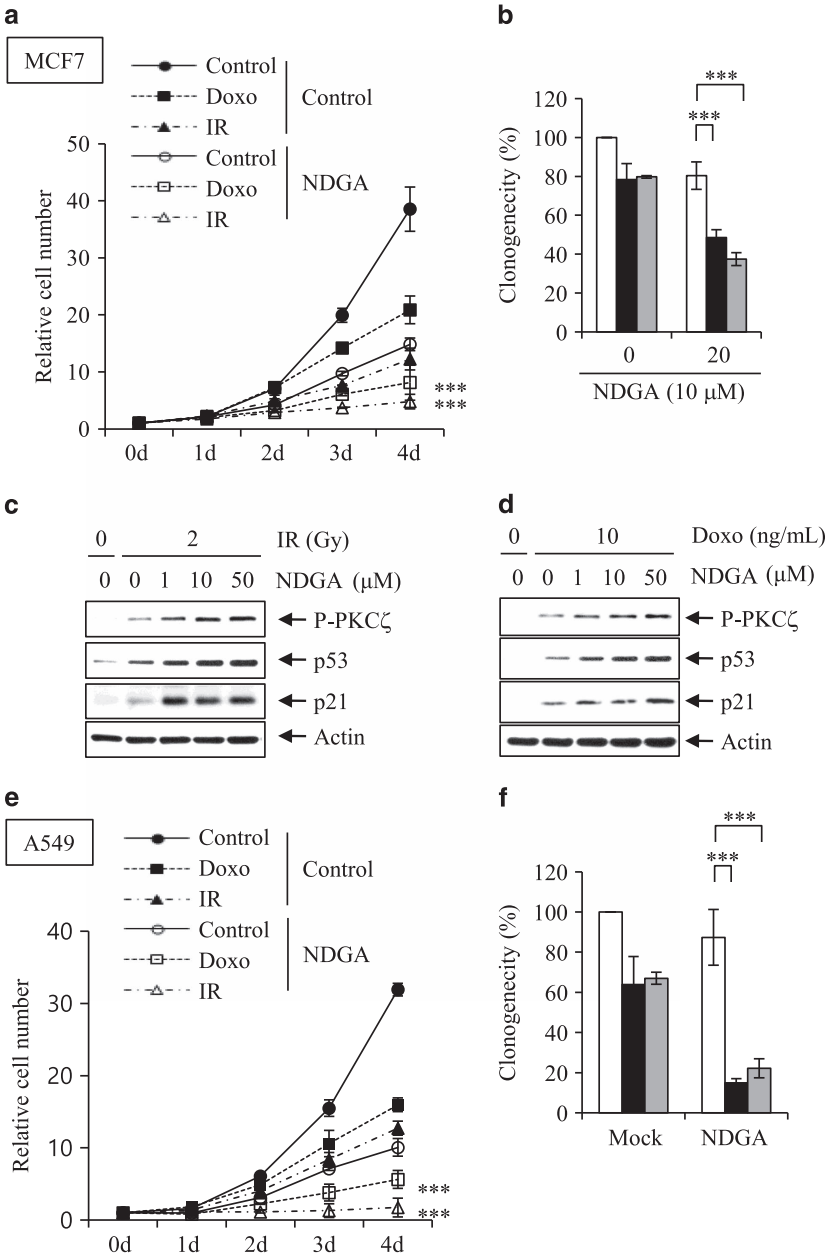

Figure 8 Synergistic anti-tumoral effect of NDGA treatment in combination with IR or Doxo. MCF7 cells were treated with NDGA prior to exposure to 2 Gy of IR or to treatment with 10 ng/ml of Doxo. (**a**–**d**) Relative cell numbers were determined at the indicated time intervals (**a**), colony-forming assay was performed at 7 days (**b**), and western blot analyses were performed in MCF7 cells 2 days (**c** and **d**) after IR or Doxo treatment. (**e** and **f**). A549 cells were treated with NDGA prior to exposure to 2 Gy of IR or treatment with 10 ng/ml of Doxo. Relative cell numbers were determined at the indicated time intervals (**e**), and colony-forming assay was performed at 7 days (**f**) after IR or Doxo treatment. NDGA concentration was 10 μM (**a**, **b**, **e**, and **f**) and actin was used as the loading control (**c** and **d**). *** and ** indicate statistical significance of $P<0.001$ and $P<0.01$, respectively, as determined by Student's *t*-test

activity of ACOT7 toward arachidonoyl-CoA may also suggest a role for thioesterase in signal transduction, possibly via PKC activation.[1] To date, however, relatively few studies have examined the pathophysiological function of ACOT7, and no study has reported the association between ACOT7 and PKCζ in cellular processes. In order to verify that activation of the PKCζ–p53–p21 signaling pathway by depletion of ACOT7 was not due to altered concentrations of free fatty acids and CoA, we depleted other members of ACOT family which are expressed in human (ACOT 1, 4, 8, 9, 11, 12, and 13) to determine their effect on cell cycle and the PKCζ–p53–p21 signaling pathway (Supplementary Figure S5). We did not include ACOT2 because it has 98% amino-acid sequence identity with ACOT1. As shown in Supplementary Figure S5, depletion of other isoforms of ACOT did not affect the PCKζ–p53–p21 signaling pathway. The results reveal that ACOT7

among the tested ACOT family members has a role in cell cycle progression through inhibition of PKCζ–p53–p21 signaling pathway.

Among ACOT family members, ACOT1 (cytosolic), ACOT2 (mitochondrial), and ACOT7 (cytosolic) have been well characterized for their enzymatic properties.[4] These ACOTs share a common feature in that their expression is markedly induced by ligands for peroxisome proliferator-activated receptor *α* (PPAR*α*), a nuclear receptor that regulates lipid metabolism-related genes such as the fibrate class of hypolipidemic drugs.[4] Moreover, ACOT1 and ACOT2 have been implicated in fatty acid catabolism, as emphasized by their upregulation in the liver and heart of fasted or high-fat-diet fed animals.[47–50] However, ACOT7 has two orders of magnitude higher enzyme activity than ACOT1 and ACOT2, and its expression is prominent in neurons of the central and peripheral nervous systems.[15,18] ACOT7 may play a role in cellular events other than energy metabolism, as overexpression of ACOT7 modified production of prostaglandins in a macrophage cell line.[9] Other members of the ACOT family that possess substrate specificity for short, medium, and long acyl-CoA were not involved in cell cycle progression through the regulation of the PKCζ–p53–p21 signaling pathway (Supplementary Figure S2d), thus implying that the role of ACOT7 might be driven by alteration of the free AA level rather than the cellular CoA level. However, secondary changes induced by ACOT7 depletion cannot be ruled out as a cause for activation of the PKCζ–p53–p21 signaling pathway. Further studies examining the molecular mechanism of ACOT7 will be required to fully determine how ACOT7 is involved in PKCζ activation and how PKCζ induces p53 accumulation.

In the present study, for the first time, we demonstrated that ACOT7 plays a critical role in cell cycle progression. ACOT7 depletion induces cell cycle arrest through regulation of the PKCζ–p53–p21 signaling pathway. We demonstrated that ACOT7 might be a valuable target for radiotherapy and chemotherapy *in vitro*. In addition, the antitumor effect of ACOT7 depletion is supported by analysis of the prognostic value and its higher expression level in lung cancer patient tissues than normal tissues. Our data reveal a non-canonical function of ACOT7 as a critical cell cycle regulator and a novel aspect of acyl-CoA thioesterase as a novel target for anticancer therapy.

Materials and Methods

Culture of cells. MCF7 and A549 cells were obtained from the American Type Culture Collection (ATCC) (Manassas, VA, USA) and grown in Dulbecco's modified Eagle's medium (PAA Laboratories GmbH, Pasching, Austria) and RPMI 1640 (WelGENE, Daegu, Korea), respectively, containing 10% FBS (Lonza Group Ltd., Basel, Switzerland) and 1% penicillin and streptomycin solution (WelGENE) at 37 °C under 5% CO_2.

Irradiation. Cells were exposed to a ^{137}Cs γ-ray source (Atomic Energy of Canada Ltd., Chalk River, Ontario, Canada) at a dose rate of 3.2 Gy/min.

Determination of relative number of viable cells. Cells were stained with trypan blue, and those excluded from staining (viable cells) were counted under a microscope using a hemocytometer. The number of viable cells prior to treatments was regarded as 1, and the number of viable cells of treatment groups were displayed as a relative number compared to the control group.

RNA interference. Sequences of siRNAs for p21, p53, and the non-specific siRNA were described previously.[51] The siRNAs for ACOT7 (5′-AGACCGAGG ACGAGAAGAAdTdT-3′), ACOT7#2 (5′-GUGCAGGUCAACGUGAUGUdTdT-3′), ACOT1 (5′-UUAAAGAAGCUGUGAACUAdTdT-3′), ACOT4 (5′-GAGAGAUUCAAG AUCAGAUdTdT-3′), ACOT8 (5′-CGAAGCUGCCAGUACUGUAdTdT-3′), ACOT9 (5′-GAUAAGUUGCGGGAGAUAGdTdT-3′), ACOT11 (5′-GCACACCAUUAGUGU UGGAdTdT-3′), ACOT12 (5′-GGUGGCUGGUCAAAAUCCAdTdT-3′), ACOT13 (5′-GAGGAAAGTCAGTGAGCAAdTdT-3′) and PKCζ (5′-GACAUGAACACAG AGGACUACCdTdT-3′) were obtained from Bioneer (Daejun, Korea). MCF7 cells were transfected with 100 nM siRNA using RNAi-MAX (Invitrogen, Carlsbad, CA, USA) according to the manufacturer's instructions.

Human tissue collection and qRT-PCR analysis. This study involving human tissues was approved by the Asan Medical Center Institutional Review Board (IRB Approval No. K-1007-002-067). Snap-frozen tissues from lung tissues were obtained from patients with lung cancer that had been diagnosed as lung adenocarcinoma, squamous cell carcinoma, or bronchioloalveolar carcinoma. Total RNA was isolated from tissues and cells using TRIzol reagent (Invitrogen). Semi-quantitative (sq) RT-PCR was performed as described previously[47] using gene-specific primers:

ACOT7, 5′-CTGCACCCTGCACGGCTTTG-3′ (sense) and 5′-CGGAAGCTGT GACGATGTTG-3′ (antisense); ACOT1, 5′-CTGCCCTAGTGGGCGTTTAG-3′ (sense), and 5′-GAACCCAAATAATCCGGCCA-3′ (antisense); ACOT4, 5′-AGGAG GGTACAAGAACCCCA-3′ (sense) and 5′- GAGGCTCGATGTAATGCCCA-3′ (antisense); ACOT8, 5′-GCCGCCTATATCTCCGACTAT-3′ (sense) and 5′-GCTCTCG CATTCATAGAGCAT-3′ (antisense); ACOT9, 5′-AAGTTCAGTGGCCATGTTAGC-3′ (sense) and 5′-AATGCCGGCCCTTTATTTTCA-3′ (antisense); ACOT11, 5′-GAGATG GTGGTGCATGTGGA-3′ (sense) and 5′-CGTCTGTACTCTGGCGTCTC-3′ (antisense); ACOT12, 5′-GCTGGAAATCTTGGTGGCTG-3′ (sense) and 5′-GCCCCAA AGCTTGACAGATG-3′ (antisense); ACOT13, 5′-CTCTTCGCCCTTTGTGTCCT-3′ (sense) and 5′-GAGTAATCTTTCCCAAAACTCTCTC-3′ (antisense) and actin, 5′-CAAGAGATGGCCACGGCT-3′ (sense) and 5′-TCCTTCTGCATCCTGTCG GC-3′ (antisense).

Immunoblot analyses. Immunoblotting was performed as described previously.[50] Briefly, whole-cell extracts or immunopurified proteins were separated on sodium dodecyl sulfate-polyacrylamide gels (6–12%) and transferred to a HyBond ECL nitrocellulose membrane (GE Healthcare, Little Chalfont, UK). The following antibodies were used as primary antibodies: anti-ACOT7 (Abcam, Cambridge, UK), anti-pRb (Cell Signaling, Danvers, MA, USA), anti-phospho-pRb (Cell Signaling), anti-cleaved PARP (Cell Signaling), anti-p53 (Do-7; Leica, Milton Keynes, UK), anti-p21 (Santa Cruz Biotech, Dallas, TX, USA), anti-cyclin D1 (Santa Cruz Biotech), anti-CDK2 (Santa Cruz Biotech), anti-CDK4 (Santa Cruz Biotech), anti-phospho-PKCα/β II(Thr638/641) (Cell Signaling), anti-phospho-PKCδ/θ (Ser643/676) (Cell Signaling), anti-phospho-PKCζ/λ(Thr410/403) (Cell Signaling), and anti-actin (Santa Cruz Biotech).

Annexin V and propidium iodide staining. Apoptosis-mediated cell death was examined using a FITC-annexin V apoptosis detection kit (BD Biosciences, San Diego, CA, USA) according to the manufacturer's instructions. Briefly, cells were incubated with 5 μl of FITC annexin V, after which 5 μl of propidium iodide (PI) was added. Stained cells were analyzed by flow cytometric analysis.

Bromodeoxyuridine incorporation assays. Incorporation of bromodeoxyuridine (BrdU) into cellular DNA was measured using a colorimetric enzyme-linked immunosorbent assay kit (Roche Applied Science, Indianapolis, IN, USA) according to the manufacturer's instructions.

Senescence associated-*β*-galactosidase staining, colony-forming activities, and cell cycles. These experiments were performed as described.[52]

Sample labeling and Illumina BeadChip array hybridization. These experiments were performed as described.[35] Array hybridizations were conducted with four sets of RNA samples from independently cultured cell samples per unit time. Array data processing and analysis was performed using Illumina BeadStudio software (Illumina. Inc., San Diego, CA, USA).

Statistical analysis. Statistical significance of values between the various experimental groups were determined using Student's two-tailed *t*-test.

Conflict of Interest

The authors declare no conflict of interest.

Acknowledgements. This work was supported by a grant awarded to J-SL from the Basic Science Research Program (No. 2014R1A2A1A11051988), Nuclear Research and Development Program (No. 2012-M2B2B1-2012055637), and Medical Research Center (MRC) (No. 201409392) through the National Research Foundation (NRF) funded by the Korean government (MSIP). This work was also partially supported by a grant from the NRF of Korea to SHJ (NRF-2015R1D1A1A01058110).

Author contributions

SHJ performed the majority of experiments and helped in writing the paper. HCL, HJH, HAP, HML, and BCK performed some experiments. KPK, Y-AM, BLL, and JCL coordinated the various collaborations and guided interpretation of the experimental data. Y-NK, Y-GK, and HJP developed ideas and provided critical discussion. J-SL conceived the study and wrote the paper.

1. Hunt MC, Alexson SE. The role Acyl-CoA thioesterases play in mediating intracellular lipid metabolism. *Prog Lipid Res* 2002; **41**: 99–130.
2. Kirkby B, Roman N, Kobe B, Kellie S, Forwood JK. Functional and structural properties of mammalian acyl-coenzyme A thioesterases. *Prog Lipid Res* 2010; **49**: 366–377.
3. Brocker C, Thompson D, Matsumoto A, Nebert DW, Vasiliou V. Evolutionary divergence and functions of the human interleukin (IL) gene family. *Hum Genomics* 2010; **5**: 30–55.
4. Ohtomo T, Nakao C, Sumiya M, Kaminuma O, Abe A, Mori A *et al*. Identification of acyl-CoA thioesterase in mouse mesenteric lymph nodes. *Biol Pharm Bull* 2013; **36**: 866–871.
5. Ellis JM, Bowman CE, Wolfgang MJ. Metabolic and tissue-specific regulation of acyl-CoA metabolism. *PloS ONE* 2015; **10**: e0116587.
6. Kang HW, Niepel MW, Han S, Kawano Y, Cohen DE. Thioesterase superfamily member 2/acyl-CoA thioesterase 13 (Them2/Acot13) regulates hepatic lipid and glucose metabolism. *FASEB J* 2012; **26**: 2209–2221.
7. Zhang Y, Li Y, Niepel MW, Kawano Y, Han S, Liu S *et al.* Targeted deletion of thioesterase superfamily member 1 promotes energy expenditure and protects against obesity and insulin resistance. *Proc Natl Acad Sci USA* 2012; **109**: 5417–5422.
8. Zhuravleva E, Gut H, Hynx D, Marcellin D, Bleck CK, Genoud C *et al.* Acyl coenzyme A thioesterase Them5/Acot15 is involved in cardiolipin remodeling and fatty liver development. *Mol Cell Biol* 2012; **32**: 2685–2697.
9. Forwood JK, Thakur AS, Guncar G, Marfori M, Mouradov D, Meng W *et al.* Structural basis for recruitment of tandem hotdog domains in acyl-CoA thioesterase 7 and its role in inflammation. *Proc Natl Acad Sci USA* 2007; **104**: 10382–10387.
10. Kang HW, Ozdemir C, Kawano Y, LeClair KB, Vernochet C, Kahn CR *et al.* Thioesterase superfamily member 2/Acyl-CoA thioesterase 13 (Them2/Acot13) regulates adaptive thermogenesis in mice. *J Biol Chem* 2013; **288**: 33376–33386.
11. Lindquist PJ, Svensson LT, Alexson SE. Molecular cloning of the peroxisome proliferator-induced 46-kDa cytosolic acyl-CoA thioesterase from mouse and rat liver–recombinant expression in *Escherichia coli*, tissue expression, and nutritional regulation. *Eur J Biochem* 1998; **251**: 631–640.
12. Svensson LT, Engberg ST, Aoyama T, Usuda N, Alexson SE, Hashimoto T. Molecular cloning and characterization of a mitochondrial peroxisome proliferator-induced acyl-CoA thioesterase from rat liver. *Biochem J* 1998; **329**: 601–608.
13. Westin MA, Alexson SE, Hunt MC. Molecular cloning and characterization of two mouse peroxisome proliferator-activated receptor alpha (PPARalpha)-regulated peroxisomal acyl-CoA thioesterases. *J Biol Chem* 2004; **279**: 21841–21848.
14. Hunt MC, Yamada J, Maltais LJ, Wright MW, Podesta EJ, Alexson SE. A revised nomenclature for mammalian acyl-CoA thioesterases/hydrolases. *J Lipid Res* 2005; **46**: 2029–2032.
15. Yamada J. Long-chain acyl-CoA hydrolase in the brain. *Amino Acids* 2005; **28**: 273–278.
16. Hunt MC, Greene S, Hultenby K, Svensson LT, Engberg S, Alexson SE. Alternative exon usage selectively determines both tissue distribution and subcellular localization of the acyl-CoA thioesterase 7 gene products. *Cell Mol Life Sci* 2007; **64**: 1558–1570.
17. Yamada J, Furihata T, Tamura H, Watanabe T, Suga T. Long-chain acyl-CoA hydrolase from rat brain cytosol: purification, characterization, and immunohistochemical localization. *Arch Biochem Biophys* 1996; **326**: 106–114.
18. Yamada J, Matsumoto I, Furihata T, Sakuma M, Suga T. Purification and properties of long-chain acyl-CoA hydrolases from the liver cytosol of rats treated with peroxisome proliferator. *Arch Biochem Biophys* 1994; **308**: 118–125.
19. Antoniotti S, Fiorio Pla A, Pregnolato S, Mottola A, Lovisolo D, Munaron L. Control of endothelial cell proliferation by calcium influx and arachidonic acid metabolism: a pharmacological approach. *J Cell Physiol* 2003; **197**: 370–378.
20. Jenkins CM, Cedars A, Gross RW. Eicosanoid signalling pathways in the heart. *Cardiovasc Res* 2009; **82**: 240–249.
21. Ellis JM, Wong GW, Wolfgang MJ. Acyl coenzyme A thioesterase 7 regulates neuronal fatty acid metabolism to prevent neurotoxicity. *Mol Cell Biol* 2013; **33**: 1869–1882.
22. Sakuma S, Fujimoto Y, Kitao A, Sakamoto H, Nishida H, Fujita T. Simultaneous measurement of prostaglandin and arachidonoyl CoA formed from arachidonic acid in rabbit kidney medulla microsomes: the roles of Zn2+ and Cu2+ as modulators of formation of the two products. *Prostaglandins Leukot Essent Fatty Acids* 1999; **61**: 105–112.
23. Fujii T, Garcia-Bermejo ML, Bernabo JL, Caamano J, Ohba M, Kuroki T *et al.* Involvement of protein kinase C delta (PKCdelta) in phorbol ester-induced apoptosis in LNCaP prostate cancer cells. Lack of proteolytic cleavage of PKCdelta. *J Biol Chem* 2000; **275**: 7574–7582.
24. Garg R, Benedetti LG, Abera MB, Wang H, Abba M, Kazanietz MG. Protein kinase C and cancer: what we know and what we do not. *Oncogene* 2014; **33**: 5225–5237.
25. Aziz MH, Manoharan HT, Church DR, Dreckschmidt NE, Zhong W, Oberley TD *et al.* Protein kinase Cepsilon interacts with signal transducers and activators of transcription 3 (Stat3), phosphorylates Stat3Ser727, and regulates its constitutive activation in prostate cancer. *Cancer Res* 2007; **67**: 8828–8838.
26. Zhao M, Xia L, Chen GQ. Protein kinase cdelta in apoptosis: a brief overview. *Arch Immunol Ther Exp* 2012; **60**: 361–372.
27. Kim KH, Nelson SD, Kim DH, Choi KU, Kim SJ, Min KW *et al.* Diagnostic relevance of overexpressions of PKC-theta and DOG-1 and KIT/PDGFRA gene mutations in extragastrointestinal stromal tumors: a Korean six-centers study of 28 cases. *Anticancer Res* 2012; **32**: 923–937.
28. Krasnitsky E, Baumfeld Y, Freedman J, Sion-Vardy N, Ariad S, Novack V *et al.* PKCeta is a novel prognostic marker in non-small cell lung cancer. *Anticancer Res* 2012; **32**: 1507–1513.
29. Sumimoto H, Kamakura S, Ito T. Structure and function of the PB1 domain, a protein interaction module conserved in animals, fungi, amoebas, and plants. *Sci STKE* 2007; **2007**: re6.
30. Terasawa H, Noda Y, Ito T, Hatanaka H, Ichikawa S, Ogura K *et al.* Structure and ligand recognition of the PB1 domain: a novel protein module binding to the PC motif. *EMBO J* 2001; **20**: 3947–3956.
31. Seidl S, Braun UB, Leitges M. Functional comparison of protein domains within aPKCs involved in nucleocytoplasmic shuttling. *Biol Open* 2012; **1**: 436–445.
32. Diaz-Meco MT, Moscat J. The atypical PKCs in inflammation: NF-kappaB and beyond. *Immunol Rev* 2012; **246**: 154–167.
33. Storz P. Targeting protein kinase C subtypes in pancreatic cancer. *Expert Rev Anticancer Ther* 2015; **15**: 433–438.
34. Coutinho I, Pereira G, Leao M, Goncalves J, Corte-Real M, Saraiva L. Differential regulation of p53 function by protein kinase C isoforms revealed by a yeast cell system. *FEBS Lett* 2009; **583**: 3582–3588.
35. Kim BC, Han NK, Byun HO, Kim SS, Ahn EK, Chu IS *et al.* Time-dependently expressed markers and the characterization for premature senescence induced by ioninzing radiation in MCF7. *Oncol Rep* 2010; **24**: 395–403.
36. Maloberti P, Lozano RC, Mele PG, Cano F, Colonna C, Mendez CF *et al.* Concerted regulation of free arachidonic acid and hormone-induced steroid synthesis by acyl-CoA thioesterases and acyl-CoA synthetases in adrenal cells. *Eur J Biochem* 2002; **269**: 5599–5607.
37. Brocker C, Carpenter C, Nebert DW, Vasiliou V. Evolutionary divergence and functions of the human acyl-CoA thioesterase gene (ACOT) family. *Hum Genomics* 2010; **4**: 411–420.
38. Broustas CG, Hajra AK. Purification, properties, and specificity of rat brain cytosolic fatty acyl coenzyme A hydrolase. *J Neurochem* 1995; **64**: 2345–2353.
39. Haq S, Kilter H, Michael A, Tao J, O'Leary E, Sun XM *et al.* Deletion of cytosolic phospholipase A2 promotes striated muscle growth. *Nat Med* 2003; **9**: 944–951.
40. Suzuki M, Boothman DA. Stress-induced premature senescence (SIPS)–influence of SIPS on radiotherapy. *J Radiat Res* 2008; **49**: 105–112.
41. Lee JJ, Kim BC, Park MJ, Lee YS, Kim YN, Lee BL *et al.* PTEN status switches cell fate between premature senescence and apoptosis in glioma exposed to ionizing radiation. *Cell Death Differ* 2011; **18**: 666–677.
42. Byun HO, Han NK, Lee HJ, Kim KB, Ko YG, Yoon G *et al.* Cathepsin D and eukaryotic translation elongation factor 1 as promising markers of cellular senescence. *Cancer Res* 2009; **69**: 4638–4647.
43. Kholodenko R, Kholodenko I, Sorokin V, Tolmazova A, Sazonova O, Buzdin A. Anti-apoptotic effect of retinoic acid on retinal progenitor cells mediated by a protein kinase A-dependent mechanism. *Cell Res* 2007; **17**: 151–162.
44. Wu HM, Schally AV, Cheng JC, Zarandi M, Varga J, Leung PC. Growth hormone-releasing hormone antagonist induces apoptosis of human endometrial cancer cells through PKCdelta-mediated activation of p53/p21. *Cancer Lett* 2010; **298**: 16–25.
45. Bluwstein A, Kumar N, Leger K, Traenkle J, Oostrum J, Rehrauer H *et al.* PKC signaling prevents irradiation-induced apoptosis of primary human fibroblasts. *Cell Death Dis* 2013; **4**: e498.
46. Sakuma S, Usa K, Fujimoto Y. The regulation of formation of prostaglandins and arachidonoyl-CoA from arachidonic acid in rabbit kidney medulla microsomes by linoleic acid hydroperoxide. *Prostaglandins Other Lipid Mediat* 2006; **79**: 271–277.
47. Yamada J, Kuramochi Y, Takoda Y, Takagi M, Suga T. Hepatic induction of mitochondrial and cytosolic acyl-coenzyme a hydrolases/thioesterases in rats under conditions of diabetes and fasting. *Metabolism* 2003; **52**: 1527–1529.

48. King KL, Young ME, Kerner J, Huang H, O'Shea KM, Alexson SE *et al.* Diabetes or peroxisome proliferator-activated receptor alpha agonist increases mitochondrial thioesterase I activity in heart. *J Lipid Res* 2007; **48**: 1511–1517.
49. Cole MA, Murray AJ, Cochlin LE, Heather LC, McAleese S, Knight NS *et al.* A high fat diet increases mitochondrial fatty acid oxidation and uncoupling to decrease efficiency in rat heart. *Basic Res Cardiol* 2011; **106**: 447–457.
50. Fujita M, Momose A, Ohtomo T, Nishinosono A, Tanonaka K, Toyoda H *et al.* Upregulation of fatty acyl-CoA thioesterases in the heart and skeletal muscle of rats fed a high-fat diet. *Biol Pharm Bull* 2011; **34**: 87–91.
51. Kim BC, Lee HC, Lee JJ, Choi CM, Kim DK, Lee JC *et al.* Wig1 prevents cellular senescence by regulating p21 mRNA decay through control of RISC recruitment. *EMBO J* 2012; **31**: 4289–4303.
52. Jung SH, Lee HC, Yu DM, Kim BC, Park SM, Lee YS *et al.* Heparan sulfation is essential for the prevention of cellular senescence. *Cell Death Differ* 2016; **23**: 417–429.

Supplementary Information accompanies this paper on Cell Death and Disease website (http://www.nature.com/cddis)